Growth of *In Situ* Functionalized Luminescent Silver Nanoclusters by Direct Reduction and Size Focusing

Madathumpady Abubaker Habeeb Muhammed,[†] Fadi Aldeek, Goutam Palui, Laura Trapiella-Alfonso,[‡] and Hedi Mattoussi*

Department of Chemistry and Biochemistry, Florida State University, 95 Chieftan Way, Tallahassee, Florida 32306, United States. [†]Present address: Department für Physik and CeNS, Ludwig-Maximilians-Universtität München, Amalienstr. 54, D-80799 München, Germany. [‡]Present address: Department of Physical and Analytical Chemistry, Faculty of Chemistry, University of Oviedo, Julian Claveria 8, 33006 Oviedo, Spain.

ABSTRACT

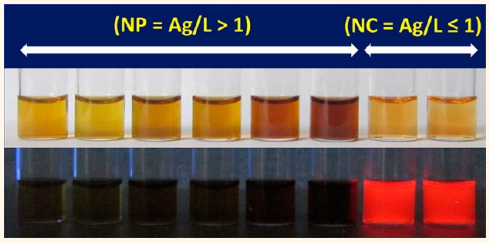

We have used one phase growth reaction to prepare a series of silver nanoparticles (NPs) and luminescent nanoclusters (NCs) using sodium borohydride ($NaBH_4$) reduction of silver nitrate in the presence of molecular scale ligands made of polyethylene glycol (PEG) appended with lipoic acid (LA) groups at one end and reactive (—COOH/—NH_2) or inert (—OCH_3) functional groups at the other end. The PEG segment in the ligand promotes solubility in a variety of solvents including water, while LAs provide multidentate coordinating groups that promote Ag—ligand complex formation and strong anchoring onto the NP/NC surface. The particle size and properties were primarily controlled by varying the Ag-to-ligand (Ag:L) molar ratios and the molar amount of $NaBH_4$ used. We found that while higher Ag:L ratios produced NPs, luminescent NCs were formed at lower ratios. We also found that nonluminescent NPs can be converted into luminescent clusters, *via* a process referred to as "size focusing", in the presence of added excess ligands and reducing agent. The nanoclusters emit in the far red region of the optical spectrum with a quantum yield of ~12%. They can be redispersed in a number of solvents with varying polarity while maintaining their optical and spectroscopic properties. Our synthetic protocol also allowed control over the number and type of reactive functional groups per nanocluster.

KEYWORDS: nanocluster · nanoparticle · luminescence · ligand · reduction · size focusing

Inorganic nanoclusters (NCs), especially those made of gold and silver, are rather a new class of nanomaterials consisting of only tens of atoms. They provide a bridge between the larger metal nanoparticles (NPs) and the molecular scale characteristics.[1] Owing to their unique optical, spectroscopic, and chemical properties, a great interest has been generated in these systems over the past few years.[1−5] For NCs, due to their very small size, the density of states is not high enough to endow them with surface plasmon resonance (SPR) features as in the case of NPs. Instead, they have discrete electronic energy levels and display "molecule-like" distinct, optical absorption and emission characteristics. NCs that exhibit size-tunable photoluminescence (PL) from the near-infrared (NIR) to the ultraviolet (UV) have been synthesized.[1,6] These materials also display two-photon absorption,[7,8] photon antibunching,[1,9] and electroluminescence.[10,11] Several applications of these NCs in areas such as nanophotonics, sensing, catalysis, and bioimaging have been demonstrated.[3,12−31] They offer a potentially new luminescent platform (or alternative) to be added to the arsenal of biological tags including organic dyes and quantum dots; they are very small, exhibit high quantum yield (QY), are photostable, and more importantly they are less affected by the "sometimes irrational" stigma of toxicity often faced by luminescent quantum dots.[32−34]

A number of methods have been reported for the synthesis of AgNCs, and the common route used reduction of Ag^+ ion precursors in the presence of suitable ligands. Various reduction techniques such as radiolytical,[35] photochemical,[36−39] sonochemical,[40] and chemical[6,41−46] have been employed. The frequently used ligands are DNA,[6,9,26,41,45,47−49] polymer microgels,[38] polyelectrolytes,[39] peptides,[50,51] proteins,[46,52] and thiol- or amine-appended molecules.[42−44,53−56] Few indiscriminately selected synthetic reports are given below. A decade ago, Dickson and coworkers prepared AgNCs by the photochemical reduction of an aqueous solution containing Ag^+ ions and a poly(amidoamine)

* Address correspondence to mattoussi@chem.fsu.edu.

Received for review July 2, 2012 and accepted September 9, 2012.

Published online September 09, 2012
10.1021/nn302954n

dendrimer, where the dendrimer acted as a cage to stabilize and solubilize the NCs, and this method produced NCs ranging from 2 to 8 silver atoms.[37] In another report, DNA templates were utilized as scaffolds for growing AgNCs, utilizing the strong affinity exhibited by Ag^+ to DNA; the addition of the reducing agent resulted in the formation of NCs with 1−4 Ag atoms bound to the 12-base oligonucleotide,[41] and the resulting NC−DNA complexes exhibited base-specific interactions. Jin and co-workers synthesized Ag_7 NCs in high yield by the reduction of $AgNO_3$ in the presence of *meso*-2,3-dimercaptosuccinic acid (DMSA) ligands.[42] A solid-state route (solvent-free) was developed to grow Ag_9 clusters starting from dry $AgNO_3$ and mercaptosuccinic acid (MSA) which were mixed and ground prior to addition of $NaBH_4$ in the solid form.[44] In addition to the direct reduction method, NCs have also been prepared from large metallic AgNPs by core etching.[53,54,57] For instance, Pradeep and co-workers synthesized two water-soluble NCs, namely, Ag_7 and Ag_8, from silver NPs by an interfacial etching reaction performed at an aqueous/organic interface.[54] Finally, Xie and co-workers reported the growth of nonluminescent NCs in water; they found that if phase transferred to toluene and incubated for 2 h the NCs become luminescent and could subsequently be transferred back to the aqueous layer.[58]

Numerous applications of AgNCs have been reported, including the sensing of biomolecules and metal ions and cellular imaging.[15,43,46,59−62] In one example, a DNA−AgNC system was developed as a substrate for the detection of a target DNA from changes in the NC luminescence; for example, a 500-fold enhancement in the NC luminescence (from a very weakly emitting starting material) was observed after hybridization with the target.[49] This technique is low cost, and the probe can attain high signal-to-background ratios upon target binding. In a second example, AgNCs synthesized *via* G-quadruplex as template were used to image cancerous HeLa cells by utilizing the ability of G-quadruplex to bind to the nucleolin, a membrane protein overexpressed in these cells.[31] It was also found that binding of G-quadruplex-capped AgNCs to nucleolin greatly enhances their luminescence properties. Another area where AgNCs found application is catalysis. For example, Ag_7 and Ag_8 NCs loaded on inorganic supports such as alumina were shown to act as catalyst for the reduction of various nitro aromatic compounds, and the supported NCs stayed active and were recycled several times after separation.[20]

Albeit the optical features are core-derived, surface ligands play a vital role in shaping the electronic properties of the NCs as most of their atoms are located at the surface. For example, glutathione-capped Au_{25} NCs and BSA-encapsulated Au_{25} NCs exhibit totally different absorption features and quantum yields even though they have the same core.[63,64] Ligands also block agglomeration, stabilize the NCs, and influence the selection of a certain thermodynamically most stable size. The colloidal stability of the nanocrystals depends on the ligand coordination onto the inorganic surface and its affinity to the surrounding solvent. For example, thiol groups are known to exhibit strong affinity to metal and semiconductor NP surfaces.

Our group has developed a number of modular ligands made of a tunable length polyethylene glycol (PEG) segment appended with lipoic acid (LA) or dihydrolipoic acid (DHLA) at one end and a potentially reactive or inert group at the other end.[65−68] These ligands were initially developed to promote the phase transfer of quantum dots (QDs) to buffer media and couple them to target biomolecules, where they provided aggregation-free, homogeneous, and reactive QD dispersions.[65,66,68] We have more recently used them to synthesize an array of gold NPs that exhibit great colloidal stability over pH ranging from strong acidic to alkaline and in the presence of excess electrolytes (up to 2 M NaCl) and dithiothreitol (DTT).[67]

Here we extend the above design and use borohydride reduction of $AgNO_3$ in the presence of LA-PEG ligands to grow both nonluminescent metal NPs and luminescent "nonmetallic" NCs of silver. Though DHLA has been previously used to synthesize AgNCs,[43] substituting LA-PEG ligands with potentially reactive terminal groups allows one to carry out the growth reaction, or redisperse already prepared NPs/NCs, in a wide range of solvents, including water. The PL of the NCs protected with LA-PEG ligands was enhanced 5-fold when compared with the NCs protected with LA alone. Furthermore, the presence of reactive end groups provides one the ability to further conjugate the NPs/NCs to various biomolecules. This will be greatly beneficial if combined with future enhancement of the long-term colloidal stability of these materials. In addition to the growth of NCs by direct reduction, we also show that polydisperse NPs can be converted to nearly monodisperse AgNCs by "size focusing" in the presence of excess ligands and reducing agent.

RESULTS AND DISCUSSION

The present design builds on our previous work where we had combined the use of LA-PEG-based ligands and one phase growth to prepare a set of AuNPs with sizes ranging from 1.5 to 20 nm in diameter.[67] Here, we wanted to extend that design to the synthesis of silver nanoparticles over a wide size range. Overall, the present study was motivated by the following objectives: (1) synthesis of an array of hydrophilic AgNPs with clearly defined size-dependent SPR bands, (2) direct growth of homogeneous and hydrophilic AgNCs with promising luminescence properties, (3) controlling the number of reactive groups per NC for subsequent functionalization, and (4) test the feasibility of transforming polydisperse nonluminescent

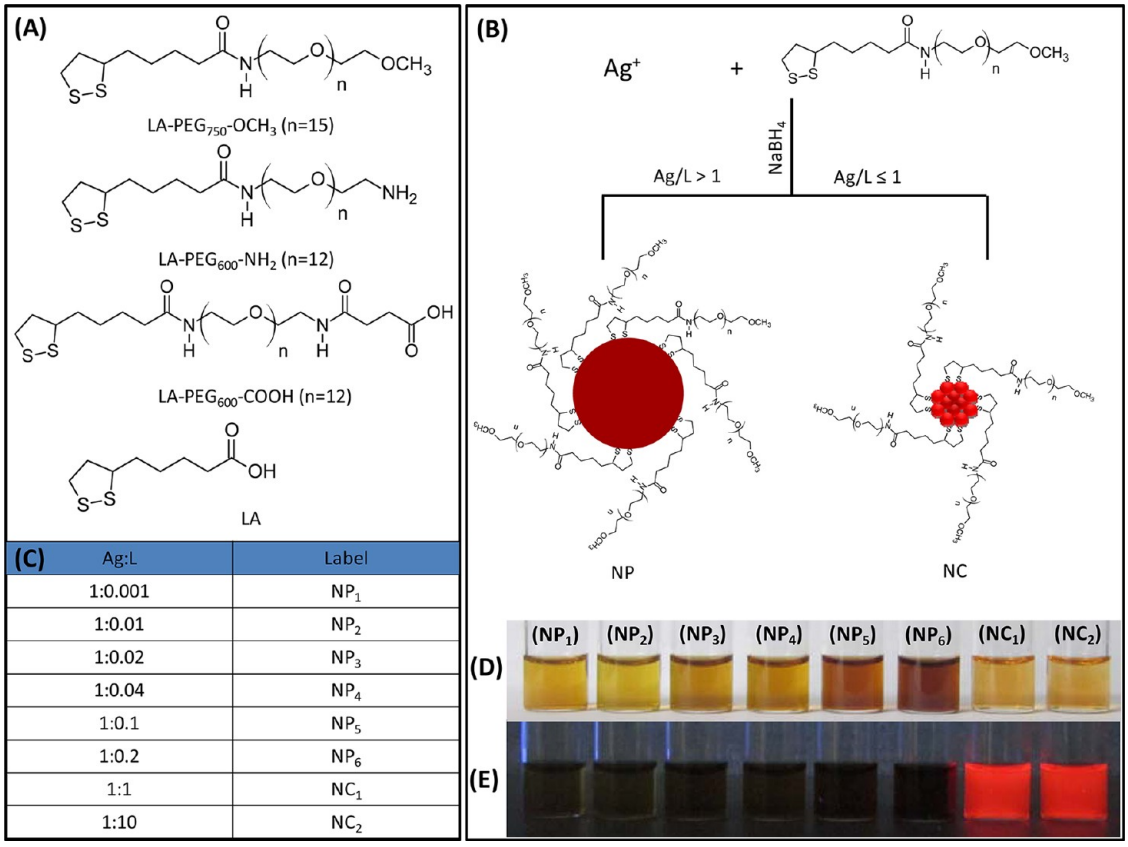

(C) Ag:L	Label
1:0.001	NP_1
1:0.01	NP_2
1:0.02	NP_3
1:0.04	NP_4
1:0.1	NP_5
1:0.2	NP_6
1:1	NC_1
1:10	NC_2

Figure 1. (A) Chemical structures of the ligands, (B) synthetic strategy of NPs/NCs of various core sizes. (C) Table showing the Ag:L ratios used for the synthesis. (D,E) Photographs of aqueous dispersions of the particles synthesized at various Ag:L ratios under room light and UV light irradiation, respectively. Images were collected from a set of freshly prepared dispersions, without filtration or adjustment of the nanoparticle or cluster concentrations.

NPs into homogeneous luminescent NCs with low size distribution and high quantum yield. Three LA-PEG-based ligands, LA-PEG_{750}-OCH_3, LA-PEG_{600}-NH_2, and LA-PEG_{600}-COOH, were prepared and used for the synthesis of NPs/NCs along with commercially available LA (see Figure 1A for their chemical structures). LA-PEG_{750}-OCH_3 was used throughout the study unless mentioned otherwise. The synthesis of NPs/NCs was carried out in two steps. First, silver nitrate ($AgNO_3$) and LA-PEG_{750}-OCH_3 were mixed in water to promote the formation of Ag-LA-PEG_{750}-OCH_3 metal−ligand complex (as a precursor), followed by the addition of $NaBH_4$ reducing agent to initiate the growth of the nanoparticles (as schematically depicted in Figure 1B). Control over the size of the resulting metal nanocrystals (NPs or NCs) was achieved by varying the Ag:L molar ratio from 1:0.001 to 1:10, while keeping the concentration of Ag ions in the reaction fixed (see the table, Figure 1C). NPs resulted for Ag:L ratios between 1:0.001 and 1:0.2, while NCs exclusively resulted for Ag:L ratios between 1:1 and 1:10 (Figure 1D,E).

Figure 2A,B shows the optical absorption spectra collected at the end of the reaction from the samples prepared with various Ag-to-L ratios. When observed under white light, the dispersions show a clear color change from yellow to dark brown to reddish brown when the Ag:L ratio decreased (see Figure 1D). The materials synthesized at Ag:L ratios ranging from 1:0.001 to 1:0.2 are NPs as indicated by the clear characteristic SPR band observed in all of the absorption spectra, which gradually red shifts with decreasing Ag-to-L ratio. For example, we measured absorption maxima at 388 for NP_1, 396 for NP_2, 398 for NP_3, 406 for NP_4, 416 for NP_5, and 434 nm for NP_6 with a gradual decrease in the absorbance value at lower Ag-to-L ratio (Figure 2A). In contrast, reactions carried out using lower ratios, namely, Ag:L = 1:1 and 1:10, produced dispersions that exhibit drastically different absorption spectra. The spectra show three prominent and well-defined absorption peaks at 330, 428, and 495 nm, along with much weaker features measured at 239, 258, and 300 nm (see Figure 2B). The well-resolved "molecule-like" absorption features are attributed to the presence of very small nanocrystals (nanoclusters, NCs) in the samples.

The two sets of dispersions, corresponding to the spectra shown in Figures 2A,B, exhibit drastically different luminescence properties as shown in Figure 2C. While NPs did not show any luminescence under any excitation wavelength, NCs exhibited pronounced luminescence with a peak centered at 680 nm. Additional proof is provided in the photograph collected

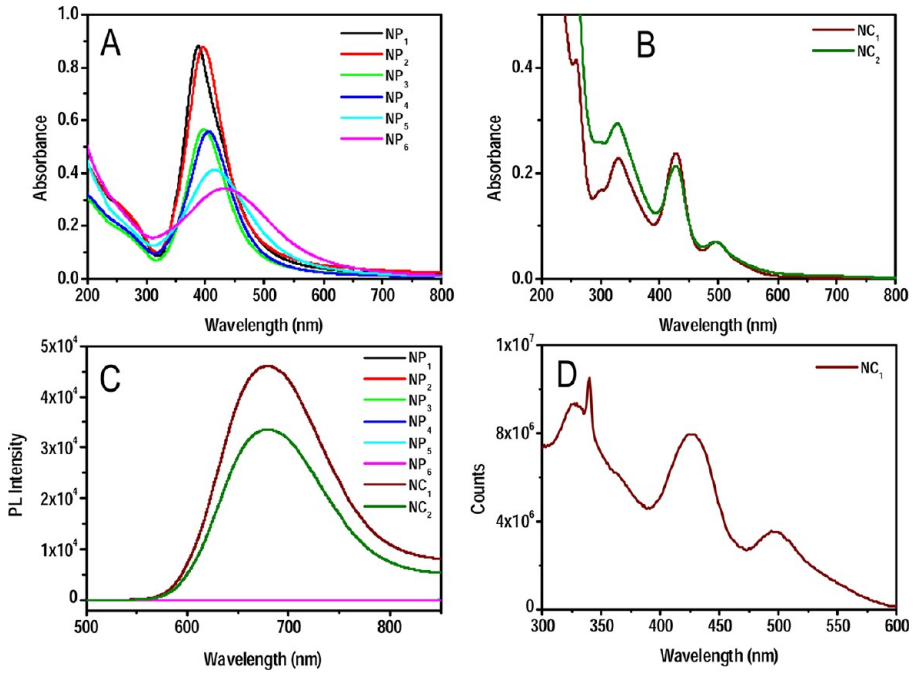

Figure 2. (A) Optical absorption spectra of NPs; (B) optical absorption spectra of NCs; (C) photoluminescence spectra of NPs and NCs at 450 nm excitation; and (D) excitation spectrum (or excitation scan) of NC_1 using detection at 680 nm. The small peak at 340 nm results from the contribution of the second overtone of the grating in the monochromator due to signal collection at 680 nm (peak of the PL spectrum).

from all of the dispersions under UV light irradiation (see Figure 1E); indeed, NP dispersions are dark, whereas the NC dispersions exhibit bright red emission. When excited at different wavelengths, the emission from NCs did not change position, albeit a change in the PL intensity, with the highest and lowest intensities measured for λ_{exc} = 330 and 495 nm, respectively (see Supporting Information, Figure S1). We should also note that the PL emission collected from dried (solid paste) NCs matched that of the dispersions. Excitation scan collected from NC_1 matched its absorption spectrum, with all three prominent absorptions featuring on both spectra (see Figure 2D). The quantum yield of the NCs in water was calculated using 4-(dicyanomethylene)-2-methyl-6-(4-dimethylaminostyryl)-4*H*-pyran (DCM) dye as reference and is found to be ~12%.

To complement the above optical and spectroscopic characterization and assign core sizes to the above dispersions, we carried out transmission electron microscopy (TEM) measurements on the following samples: NP_2, NP_3, NP_4, NP_5, and NC_1 (see Figure 3 and 7B for NP_4). The TEM images collected from NP_2, NP_3, and NP_4 showed that the particles exhibit large size dispersity, while the image of NP_5 showed nanoparticles with substantially lower size distribution. As for NC_1, the image shows more homogeneous nanocrystals with a core size of ~1.3 nm. Overall, on the basis of the absorption properties combined with the TEM data, we conclude that larger metallic NPs which exhibit clearly defined SPR are formed at high Ag-to-ligand ratios (Ag:L = 1:0.001 to 1:0.2) while smaller nonmetallic and luminescent NCs are formed at low ratios (Ag:L = 1:1 to 1:10). Similar correlations between metal-to-L ratio and nanocrystal size were also observed for the growth of AuNPs using this same growth reaction and the same ligands.[67]

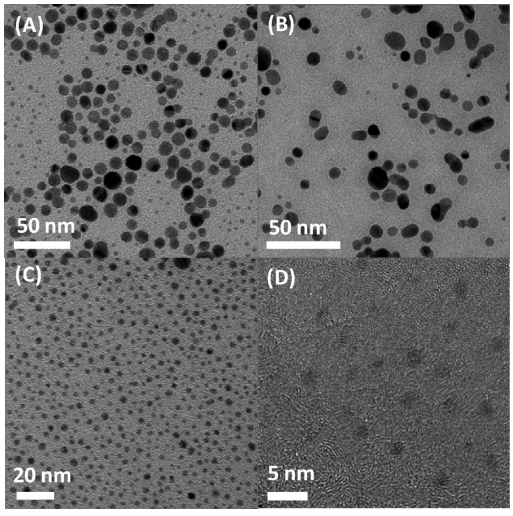

Figure 3. Transmission electron microscopic images of (A) NP_2, (B) NP_3, (C) NP_5, and (D) NC_1. Images clearly show the size progression with changes in the Ag-to-ligand ratios used.

We also synthesized NCs protected with lipoic acid. For this, a sodium salt of LA is made first by adding the base NaOH since LA is insoluble in water. LA-protected NCs showed all of the absorption features and similar absorbance values, albeit a slight wavelength shift for

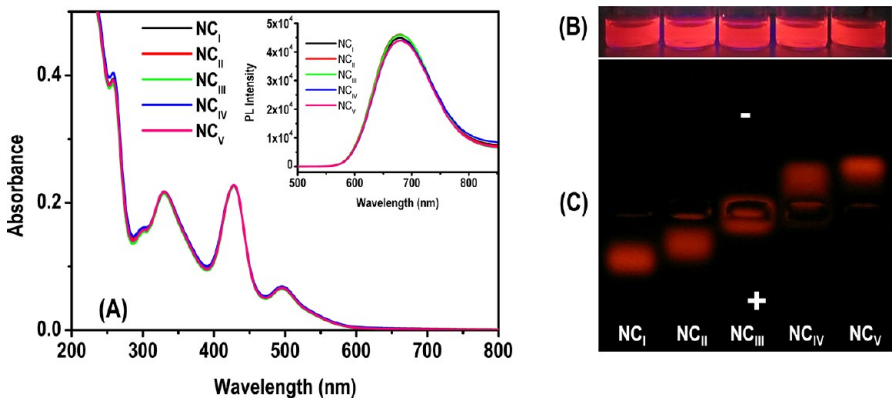

Figure 4. (A) Optical absorption spectra of NCs capped with ligands of different functionalities, namely, 100% LA-PEG-COOH (NC_I), 50% LA-PEG-COOH and 50% LA-PEG-OCH_3 (NC_{II}), 100% LA-PEG-OCH_3 (NC_{III}), a mixture of 50% LA-PEG-NH_2 and 50% LA-PEG-OCH_3 (NC_{IV}), and 100% LA-PEG-NH_2 (NC_V). Inset shows the corresponding photoluminescence upon 450 nm excitation. (B) Photograph of the aqueous dispersions of the NCs upon UV excitation using a hand-held UV lamp. (C) Gel electrophoresis image of the above dispersions under UV light irradiation; the red color results from the NC emission.

the main absorption features (330, 426, 496 nm), when compared with NCs synthesized using PEGylated ligands. However, these NCs exhibited a slightly red-shifted (~17 nm) luminescence, and the measured intensity was ~5 times smaller than LA-PEG-protected NCs (QY ~3.3%; see Supporting Information, Figure S2). This suggests that equal numbers of NCs are formed, but the larger ligand structure of the LA-PEG enhances the luminescence from these materials. When compared with our data, DHLA-capped AgNCs synthesized by Banerjee and co-workers exhibited absorption features at 335, 435, and 500 nm and emission at 652 nm.[43]

Remark: We have attempted mass spectrometry characterization using both electrospray ionization (ESI) and matrix-assisted laser desorption ionization (MALDI) techniques in order to possibly assign a chemical composition to these NCs. No reliable information was obtained. We observed only peaks corresponding to the ligand in both cases (see Supporting Information, Figure S3). This may be due to the inadequacy of the commonly used matrices and the limited stability of the AgNCs even under the soft ionization conditions.[57]

Our one phase growth route affords the ability to control the surface functionalities of the NCs *in situ*. This can be achieved by mixing inert LA-PEG-OCH_3 ligands with reactive LA-PEG-COOH and/or LA-PEG-NH_2 ligands during the growth reaction.[66,69] We have synthesized five batches of NCs by mixing $AgNO_3$ precursor with the following ligand combinations (Ag:L = 1:1): 100% LA-PEG-COOH (NC_I), 50% LA-PEG-COOH and 50% LA-PEG-OCH_3 (NC_{II}), 100% LA-PEG-OCH_3 (NC_{III}), 50% LA-PEG-NH_2 and 50% LA-PEG-OCH_3 (NC_{IV}), 100% LA-PEG-NH_2 (NC_V). In all cases, the formed NCs exhibited identical absorbance values and similar luminescence intensities to those shown above (see Figure 4A and inset of 4A); the photograph of the NC dispersions under UV excitation, as shown in Figure 4B, further confirms that comparable luminescence is generated from all of the samples. The NCs capped with different functional groups exhibited a QY of ~12%. This result suggests that the growth of NCs is not affected by the ligand end functionality, a property directly attributable to the fact that all of these ligands have a similar PEG structure and exhibit the same affinity toward the nanocrystal surfaces.

The gel image shown in Figure 4C demonstrates that while NC_{III} (grown with 100% LA-PEG-OCH_3) did not exhibit any mobility shift, NC_I, NC_{II}, NC_{IV}, and NC_V (grown with $-$COOH, OCH_3/COOH, OCH_3/NH_2, and $-NH_2$) experienced a ratio-dependent mobility shift; NC_I (100% LA-PEG-COOH) and NC_V (100% LA-PEG-NH_2) experienced the largest mobility shift. Furthermore, the sign of the displacement varied with the nature of the functional groups, confirming the presence of negative charges for carboxyl-terminated ligands (migration toward the anode) and positive charges for aminated ligands since the NCs migrated toward the cathode. The achieved control over NC functionality is of great importance, as this would help one to tune the reactivity of the NP/NC and allow further functionalization with target molecules such as proteins, peptides, and DNAs. This procedure can be extended to NPs to prepare surface-functionalized AgNPs.[67]

Our long-term colloidal stability tests indicate that the integrity of the NCs (as prepared in aqueous dispersion, pH ~10) is preserved for several months when protected from light. However, the clusters progressively lose their characteristic absorption and emission features when exposed to direct sun light or UV irradiation (see Supporting Information, Figure S4). The reason for the photosensitivity is unknown as of now. We also checked the stability of the NC dispersions over a broad range of pH values in the presence of excess NaCl or growth media (see Supporting Information, Figure S5). Data indicate that the NCs

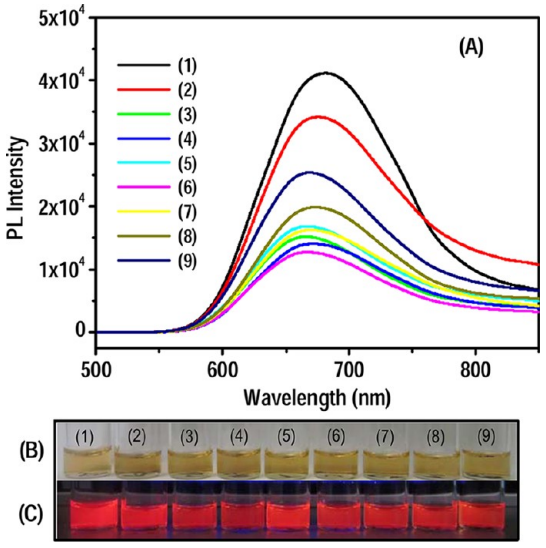

Figure 5. (A) PL spectra of AgNCs redispersed in different solvents: (1) water, (2) chloroform, (3) acetone, (4) acetonitrile, (5) THF, (6) DMF, (7) ethyl acetate, (8) methanol, and (9) 2-propanol. Images (B) and (C) show photographs of the dispersions in various solvents under room light and UV light irradiation using a hand-held UV lamp, respectively.

exhibit long-term stability only in basic buffers. Conversely, the NCs are stable in the presence of 1 M NaCl for at least one week, but emission is essentially lost after one day of storage in cell culture media (Dulbecco's modified Eagle media, DMEM).

Transfer of the NPs and NCs from one medium to another is very important as it can indicate one's ability to process these materials from various solution conditions and potentially develop tailor-designed applications requiring the availability of the materials in solvents with drastically different properties. In addition, the environment surrounding a fluorophore (*e.g.*, solvent) often plays an important role in determining the luminescence intensities and sometimes the emission wavelength.[22,70] To check the solubility of the NCs in different solvents, the native aqueous dispersion was first lyophilized and the resulting paste was dissolved in chloroform; then aliquots of this dispersion were transferred to open vials, and the solvent was allowed to evaporate in the dark. After the complete solvent removal, water, chloroform, acetone, acetonitrile, THF, DMF, ethyl acetate, methanol, and 2-propanol were added in equal amounts to each vial, then absorption and PL sepctra were collected. The measured absorption spectra exhibited all of the prominent absorption features of the NCs; absorption spectra in some selected solvents are provided in the Supporting Information (Figure S6). There was, however, a partial loss in the PL emisson and a slight change in the peak location in certain solvents (Figure 5A). For instance, the peak emission measured in acetone was slightly blue-shifted compared to water (peak at 663 nm compared to 680 nm in water). The QY values of the NCs in these solvents are provided in the Supporting Information, Table S1. Figure 5B,C shows a photograph of the NC dispersions in different solvents under white light and UV light irradiation, respectively. The solubility of the NCs in different solvents can primarily be attributed to the affinity of the ligands to those media. We should note that after two weeks of storage, only dispersions in water, 2-propanol, acetonitrile, and DMF retained their emission; substantial losses were measured in other solvents.

The absorption spectra collected from samples NP_1 to NP_6 (prepared using excess molar of Ag) consistently showed well-defined broad single absorption peaks located at 390−430 nm. We attribute this peak to surface plasmon resonance (SPR, ascribed to the coherent oscillations of electrons near the NP surfaces), as widely reported for Ag nanoparticles prepared *via* other growth routes.[71] However, the multiple absorption features in the spectra collected from the clusters (NC_1 and NC_2, synthesized using equal or higher molar concentration of LA-PEG ligands) cannot be attributed to SPR. These samples are made of much smaller size nanocrystals, as evident from the TEM image, and they do not have enough electron densities to support SPR characteristics, as their larger size NP counterparts do. Instead, they contain much smaller numbers of atoms and display discreet *molecule-like* absorption peaks. In general, NCs of gold and silver exhibit multiple absorption features throughout the UV−vis region, though those features are not as well-defined and understood as those measured for semiconductor QDs. Preceding reports about the time-dependent density functional theory (TDDFT) calculations of the electronic structures and optical spectra of the NCs indicate that the absorption features result from the electronic transitions between the molecular orbitals (MOs) of the clusters.[72,73] TDDFT calculations of NCs help us to understand how the nature of electronic and optical properties vary with size, geometry, and chemical environment such as nature of the ligand coordination onto the NC surface. Aikens and co-workers conducted TDDFT calculations to determine the optical absorption spectra for a series of silver clusters (Ag_n, n = 6−85) with various charge states.[74] Those clusters exhibit octahedral, truncated octahedral, and icosahedral structures. In the absence of a structural model (crystal structure or geometry) at the moment for our NCs, we cannot assign each absorption feature to a particular electronic transition, as was done in refs 72 and 73. However, we can propose a general qualitative explanation for the origins of the absorption features measured for our luminescent NCs. For AgNCs, the MOs are mainly made up of Ag (5sp), Ag (4d) atomic orbitals of the core and sulfur (S), 3p atomic orbital of the ligand.[73] MOs made up of sp orbitals constitute the sp band, whereas those made up of d orbitals constitute the d band. All of the MOs have contribution from the sulfur 3p orbital of the ligand, indicating that the optical absorption

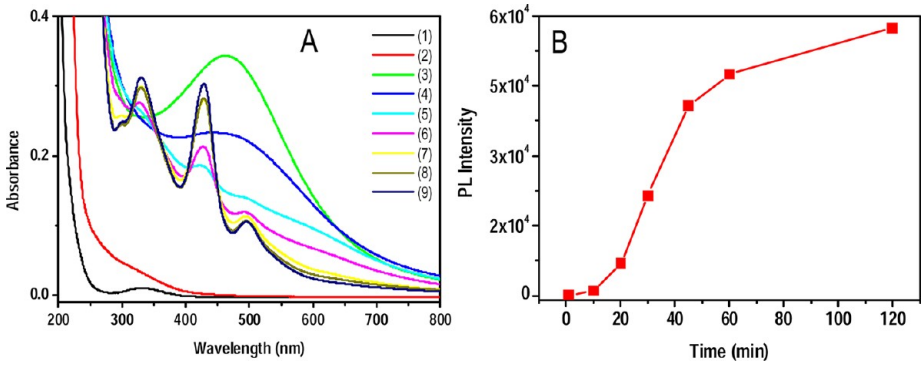

Figure 6. (A) Time-dependent optical absorption spectra during AgNC synthesis. Absorption spectra of ligand alone (1), after the addition of Ag precursor (2), then 5 min (3), 10 min (4), 20 min (5), 30 min (6), 45 min (7), 1 h (8), and 2 h (9) after the addition of $NaBH_4$ to the mixture. (B) Plot of PL intensity *vs* time during the NC synthesis.

spectrum is a combination of core and ligand contributions.[75] Ligand contribution may play a larger role here since the absorption features measured for the clusters prepared in the presence of lipoic-based ligands are different from what has been reported for monothiol-alkyl ligands. It is believed that low-energy/high-wavelength optical features are due to intraband sp to sp transitions, and high-energy/low-wavelength features result from interband d to sp transitions.

The luminescence measured for our NCs results from the relaxation of the excited electron back into the ground state (HOMO) across the energy barrier (gap). The single color emission may be attributed to a combination of single average size NCs afforded by our reaction scheme and band edge emission. Electrons excited to higher energy states always rapidly relax nonradiatively to the band edge before recombining with the hole in the HOMO, emitting red photons. This process is similar to the PL generated from semiconductor nanocrystals.[76]

We now focus on elucidating the mechanism of NC growth *via* either of the routes described in the Experimental Section, namely, direct reduction of Ag precursor or size focusing of nonluminescent nanoparticles. For the direct reduction route, we first monitored the absorption spectrum of the ligand mixed with $AgNO_3$ in the absence of borohydride. We found that a weak peak is measured at ~330 nm for the free ligand, which rapidly disappeared when $AgNO_3$ was added (see Figure 6A). The resulting solution became colorless and exhibited no photoluminescence. Five minutes after the addition of $NaBH_4$, the solution turned dark brown and a broad peak centered at 463 nm appeared. After 10 min, the peak broadens and its absorbance decreases and then gradually resolves into three prominent absorption features with time. The above transformation of the absorption spectrum after the addition of borohydride was accompanied by a gradual build up in red fluorescence (see Figure 6B), and the reaction was complete within ~2 h when both absorption and emission spectra reached saturation.

The weak absorption peak of the free ligand at ~330 nm is due to the strained five-membered cyclic disulfide structure of lipoic acid.[77] When silver nitrate is added, the Ag^+ ions progressively complex with the disulfide group (due to the affinity exhibted by this group to several metals, including Au and Ag) to form the Ag-LA-PEG metal−ligand complex, referred to as the precursor.[67] During this procedure, the disulfide bond is weakened, leading to the disappearance of the peak at 330 nm; no NCs are formed at this time. After the addition of $NaBH_4$, reduction of Ag-LA-PEG complex to Ag(0) initiates the growth of Ag cores, likely over broad size range;[63,78−80] these Ag cores have different stabilities, and they slowly convert with time into a single average and thermodynamically stable NC. Since the molar concentration of Ag is fixed during the reaction, equilibrium favoring smaller size NCs requires much higher concentration of stabilizing ligands in order to accommodate their higher surface-to-volume ratio and larger number. In comparison, at lower ligand concentration, equilibrium favors the growth of larger size NPs where the overall area to be passivated is smaller. Growth of NCs also depends on the amount of reducing agent. A minimum of 5-fold excess of reducing agent (in terms of Ag^+ precursor concentration) is required to form clusters. Maximum luminescence is observed when 20-fold excess of $NaBH_4$ is used.

Finally, we confirmed that the absorption and emission features of the NCs are core-derived by carrying out an etching experiment using CN^- ions. Cyanide ions are known to convert Ag(0) to AgCN by the core etching of NPs.[54,81] An aqueous dispersion of NCs was mixed with a molar excess of sodium cyanide and left to stir overnight. We found that such treatment leads to the disappearance of all of the absorption features as well as the PL signal, while the solution turned colorless, suggesting that cyanide ions dissolved the core silver, resulting in the collapse of the NCs.

In the second synthesis route, referred to as size focusing, polydisperse larger size NPs are converted into homogeneous smaller size NCs; this process is also

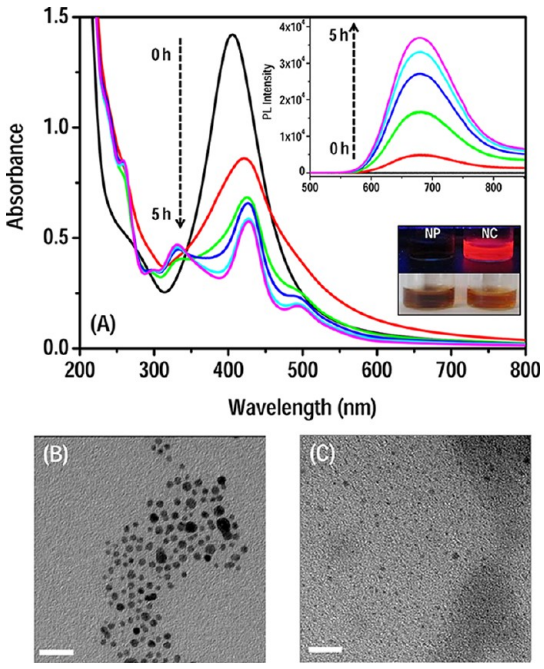

Figure 7. (A) Time-dependent evolution of optical absorption features of NCs during the size focusing of NP_4 (initially synthesized using 1:0.04 Ag:L molar ratio). Inset shows the corresponding emission spectra. The photograph of the NP before and after size focusing under bright light and UV light is also shown. TEM images of AgNPs (B) before and (C) after size focusing. The scale bar designates 20 nm.

known as "core etching" in the literature. To follow the synthesis using this method, we tracked the time progression of the optical characteristics (absorption and emission) of a NP dispersion (prepared using Ag:L = 1:0.04, NP_4) after mixing with excess ligands and $NaBH_4$. Aliquots from the reaction mixture were retrieved, and spectra were collected at regular intervals. Figure 7A shows that the initial NP dispersion exhibits an SPR band located at 406 nm and no luminescence. After addition of the ligand and $NaBH_4$, the band progressively decreased and red-shifted with time; for example, the SPR peak shifted to 418 nm, and the solution showed a very weak emission at 680 nm after 15 min. As time progressed, these changes continued to develop until the complete disappearance of the SPR peak was replaced with the characteristic absorption features of the NCs; these changes were accompanied with an enhancement in the measured luminescence (see Figure 7A). The color of the NP dispersion changed from dark brown with no luminescence (before) to reddish brown with bright luminescence after size focusing (Figure 7A, inset). Saturation of the absorption and emission spectra was reached after 3−5 h from the addition of ligand and reducing agent. This change in optical features and the evolution of emission indicate the formation of NCs.

We further confirmed the complete conversion of a rather polydisperse NP population into homogeneous NCs using TEM. The TEM image of as-grown NPs showed nanoparticles with a rather broad size range (∼7−2 nm, Figure 7B). Following size focusing, the larger particles progressively disappeared, replaced with a homogeneous population of nanocrystals having an average diameter of ∼1.3 nm (see Figure 7C).

Size focusing required the addition of a large amount of the ligands (comparable to the amounts used for NC growth by direct reduction). In the absence of $NaBH_4$, no characteristic absorption features or emission of NCs was observed after several hours even in the presence of ligands. Similarly, in the absence of ligands, no visible change in the SPR band of the NP was observed. We also found that while the smaller size NPs (synthesized at 1:0.02 to 1:0.2 Ag:L ratios) exhibited size focusing, NPs synthesized at 1:0.001 and 1:0.01 ratios (larger size NPs) did not (see Supporting Information, Figure S7). They only showed a slight red shift and a decrease in absorbance of the SPR band at all times. Overall, we found that at least 5-fold molar excess of $NaBH_4$ and a final Ag:L = 1:1 or higher are required to achieve complete transformation of NPs into luminescent clusters.

We would like to emphasize that size focusing can be carried out using a mixture of inert and end-functionalized ligands, which indicates that surface-functionalized NCs can also be prepared using this route (NP growth and size focusing). For instance, we performed this procedure on NPs previously synthesized at 1:0.1 Ag:L ratio with ligands made of 100% −COOH (NC_{SI}), 50−50 mixture of $-OCH_3$ and −COOH (NC_{SII}), 100% $-OCH_3$ (NC_{SIII}), 50−50 mixture of $-OCH_3$ and $-NH_2$ (NC_{SIV}), and 100% of NH_2 (NC_{SV}) separately. The reaction was allowed to continue for equal time for the five batches. All of the resulting dispersions exhibited characteristic absorption features of NCs with the same absorbance values and PL intensities (see Figure 8A,B). This suggests that ligands of any functionality can be used, and the populations of the NCs formed at the end of the reaction are essentially identical. Additionally, gel electrophoresis experiments showed that while NC_{SIII} (obtained with 100% LA-PEG-OCH_3) did not exhibit any mobility shift under applied voltage, all of the other NCs showed shifts with the expected sign and magnitude, due to the presence of either −COOH or $-NH_2$ (see Figure 8C).

Even though the mechanism that drives the conversion of NPs to NCs is not clearly understood, a tentative explanation can be provided. The initial growth step provides NPs with a broad size range, and their surface-to-volume ratio and thermodynamic stability vastly differ. For NP synthesis, the ratio of Ag-to-L is high, which means that the number of ligands on their surface is low and hence can be less stable. When excess ligands are provided (to a final Ag:L ratio of 1:1, identical to those used in the direct reduction method), the free thiols can progressively "etch" the NPs, leading to reduction in size and polydispersity,

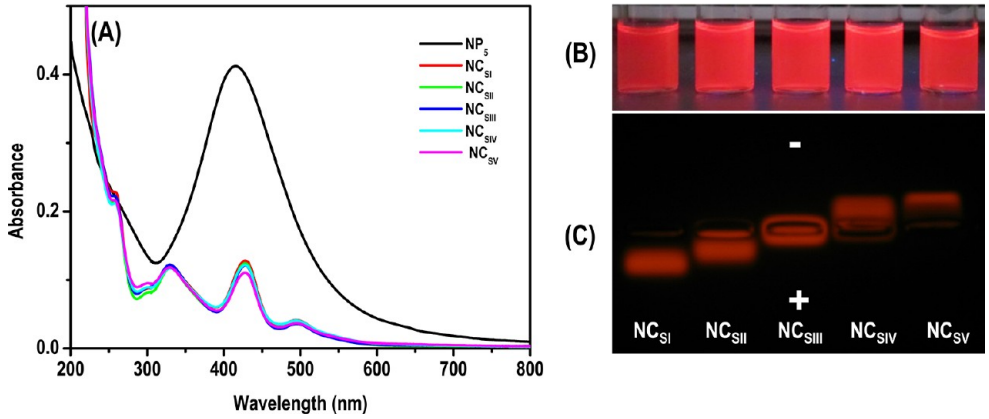

Figure 8. (A) Optical absorption spectra of the NCs formed after size focusing with ligands of different end functionalities: 100% LA-PEG-COOH (NC_{SI}), 50% LA-PEG-COOH and 50% LA-PEG-OCH_3 (NC_{SII}), 100% LA-PEG-OCH_3 (NC_{SIII}), a mixture of 50% LA-PEG-NH_2 and 50% LA-PEG-OCH_3 (NC_{SIV}), 100% TA-PEG-NH_2 (NC_{SV}), and the parent NP_5 (synthesized at 1:0.1 Ag-to-L ratio). (B) Photograph of the aqueous dispersion of the samples upon UV light irradiation and (C) gel electrophoresis image.

providing a homogeneous dispersion of smaller size clusters.[53,54,57,78,82]

CONCLUSION

We have synthesized an array of NPs and NCs of silver using ligands made of a tunable length polyethylene glycol segment appended with lipoic acid at one end and a potentially reactive (−COOH/−NH_2) or inert group (−OCH_3) at the other end. The particle size was controlled by varying the Ag-to-ligand ratio. While higher Ag-to-ligand ratio promoted the formation of NPs, lower ratios favored the formation of NCs. We also showed that the as-synthesized polydisperse nonluminescent NPs can be "size focused" to a homogeneous population of luminescent nanoclusters. This implies that the NCs can be synthesized by two routes: a one-step direct reduction of Ag^+ ions (bottom-up) or a two-step size focusing (top-down) starting from nonluminescent nanoparticles.

Our tailor-made ligands offer manifold advantages. The presence of PEG segments considerably enhances the photophysical properties such as quantum yield of NCs in addition to solubility in a wide range of solvents. The resulting NPs and NCs can be easily transferred from aqueous to organic solutions, without requiring cap exchange as is done with most other materials (*e.g.*, those prepared *via* a citrate reduction). This broad solubility may help in expanding the utility of these clusters in other areas such as catalysis. Lipoic acid offered multidentate coordination and helped in the Ag−ligand precursor formation. Our synthetic route affords the ability to control the number of functional groups on the NC surface by mixing inert and functional ligands during the growth. This opens up new opportunities for these NCs in biological applications such as imaging and sensing; nonetheless, this potential still hinges on the ability to improve the long-term stability of the PL emission of these materials. Finally, our synthetic design should be easily extended to other nanoclusters such as gold, copper, and palladium.

EXPERIMENTAL SECTION

Materials. Poly(ethylene glycol) (molecular weight average of 600), poly(ethylene glycol) methyl ether (molecular weight average of 750), methanesulfonyl chloride, triphenylphosphine, lipoic acid (thioctic acid), DMAP (4-(*N*,*N*-dimethylamino)pyridine), DCC (*N*,*N*-dicyclohexylcarbodiimide), triethylamine, sodium borohydride, succinic anhydride, NaOH, KOH, $NaHCO_3$, organic solvents, PBS buffer, and salts (such as NaCl, Na_2SO_4, Mg_2SO_4) were purchased from Sigma Chemicals (St. Louis, MO). Sodium azide and silver nitrate were purchased from Alfa Aesar (Ward Hill, MA). The chemicals and solvents were used as purchased unless otherwise mentioned. Deuterated solvents were purchased from Cambridge Isotope Laboratories (Andover, MA). Column purification chromatography was performed using silica gel (60 Å, 230−400 mesh, from Bodman Industries, Aston, PA).

Instrumentation. ^{1}H NMR spectra of all compounds were recorded using a Bruker SpectroSpin 600 MHz spectrometer. The optical absorption measurements were carried out using a Shimadzu UV−vis absorption spectrophotometer (UV 2450 model), while the luminescence spectra were collected on a Fluorolog-3 spectrometer (Jobin Yvon Inc., Edison, NJ) equipped with PMT and air-cooled CCD detectors. The emission spectra were collected using the CCD detector, whereas the excitation spectra were collected using the PMT. Transmission electron microscopy (TEM) images were taken using a 200 kV JEOL-2010 instrument or a Philips FEI CM-120 operating at an acceleration voltage of 120 kV. Samples for TEM were prepared by drop casting the NP/NC dispersion onto the holey carbon film on a fine mesh Cu grid (400 mesh) and letting it dry. Gel electrophoresis experiments were run on a 1% agarose gel. The NC dispersions were first diluted in a 10% glycerol 1× TBE Tris borate EDTA (100 mM Tris, 83 mM boric acid, 1 mM EDTA, pH 8.3) loading buffer. Aliquots of these dispersions were loaded into 1% agarose gel, and mobility shift experiments were conducted using an applied voltage of 7−8 V/cm for 15 min. The gel was imaged using a UVP transilluminator equipped with a digital camera.

Synthesis of LA-PEG Series. Three ligands made of a polyethylene glycol segment appended with lipoic acid at one end and

potentially reactive (−COOH/−NH_2) or inert (−OCH_3) groups at the other end were synthesized, purified, and characterized according to our previous synthetic protocols.[66,69,83] They are LA-PEG_{750}-OCH_3 (PEG MW = 750), LA-PEG_{600}-COOH (PEG MW = 600), and LA-PEG_{600}-NH_2 (PEG MW = 600).

Growth of Silver Nanoparticles (AgNPs). Nanoparticles were typically grown when borohydride reduction of $AgNO_3$ precursor was carried out using rather large silver-to-ligand molar ratios (Ag:L ranging from 1:0.001 to 1:0.2). This was achieved by varying the molar concentration of the ligand while maintaining that of $AgNO_3$ fixed. In a typical synthesis, 30 μL of 5 mM $AgNO_3$ and the desired molar concentration of LA-PEG_{750}-OCH_3 were dissolved in 3 mL of deionized water. The mixture was stirred at room temperature for 15−30 min to promote precursor formation, then 30 μL of 50 mM $NaBH_4$ was added, followed by stirring for another 1 h. Once the reaction was complete (*i.e.*, when no change in the absorption features could be measured), excess free ligands were removed by centrifugation using a 10 kDa membrane filter, and the dispersion was used for further characterization. Different combinations of ligands such as LA-PEG_{750}-OCH_3 (inert), end-functionalized (namely, LA-PEG_{600}-NH_2 or LA-PEG_{600}-COOH), or mixtures of the two or three can be used to synthesize surface-functionalized NPs.

Growth of Silver Nanoclusters (AgNCs) *via* Direct Borohydride Reduction. As done above for growing NPs, we maintain the amount of Ag precursor fixed (30 μL of 5 mM $AgNO_3$) and vary the molar concentration of LA-PEG_{750}-OCH_3 in 3 mL of deionized water; typically, the range of Ag-to-LA-PEG ratio could be varied between 1:1 and 1:10. Following precursor formation, 30 μL of 100 mM $NaBH_4$ was added with stirring, and the mixture was then left stirring for 2 h. Excess free ligands were removed by centrifugation using a 10 kDa membrane filter. The reaction was carried out under dark or was protected from light. Here also, the ligand LA-PEG_{750}-OCH_3 can be replaced with LA-PEG_{600}-NH_2 or LA-PEG_{600}-COOH or a mixture of the two to synthesize functionalized NCs. Growth of AgNCs was also carried out in various organic solvents including methanol, ethanol, chloroform, 2-propanol, and THF.

Preparation of Silver Nanoclusters *via* Size Focusing Starting from AgNPs. This procedure involves the progressive transformation of larger size (naturally polydisperse) NPs into a set of smaller size NCs (nearly monodisperse).[78,80,82,84] This process is also referred to as core etching in the literature. For this, aqueous dispersions of freshly synthesized NPs were further treated with additional (excess) ligands and $NaBH_4$. The amount of ligands added was such that the final Ag:L ratio (initial and added) in the sample was 1:1, while the concentration of $NaBH_4$ was 5-fold that of the ligand added for size focusing. The solution was left stirring at room temperature, and the reaction was monitored by retrieving aliquots at regular intervals and collecting the optical absorption and emission spectra. The reaction was stopped after 3−5 h when there was no further change in the optical absorption and emission spectra. The solution was centrifuged (at 20 000 rpm) for 30 min followed by filtration with a 50 kDa membrane filter. Excess ligands were removed by the subsequent filtration with a 10 kDa membrane filter.

Quantum Yield Measurement. Quantum yield (QY) values of NCs with different ligands and in different solvents were calculated using 4-(dicyanomethylene)-2-methyl-6-(4-dimethylaminostyryl)-4*H*-pyran (DCM) dye as the standard (ST). We have used the following equation, $QY_{NC} = QY_{ST}(I_{NC}/A_{NC})(A_{ST}/I_{ST})(\eta_{NC}/\eta_{ST})^2$, where I, A, and η are the integrated emission intensity, absorbance at excitation wavelength, and refractive index of the solvent, respectively. Optical densities of the NC dispersion and DCM solution were adjusted below 0.1 at the excitation wavelength of 450 nm. DCM was dissolved in methanol, and its QY is reported to be 43%.

Conflict of Interest: The authors declare no competing financial interest.

Acknowledgment. The authors thank FSU, the National Science Foundation (NSF-CHE, Grant No. 1058957), and Pfizer for financial support. We also thank Xin Ji, Naiqian Zhan, and Dr. Lei Bruschweiler for the helpful discussions and assistance with the gel experiments.

Supporting Information Available: Additional experimental details on the cluster growth using lipoic acid, a MALDI-MS spectrum, UV−vis Abs and/or fluorescence emission from dispersions following exposure to UV and white light, progression of the Abs and emission spectra during size focusing experiments, quantum yield values, and colloidal stability tests. This material is available free of charge *via* the Internet at http://pubs.acs.org.

REFERENCES AND NOTES

1. Zheng, J.; Nicovich, P. R.; Dickson, R. M. Highly Fluorescent Noble-Metal Quantum Dots. *Annu. Rev. Phys. Chem.* **2007**, *58*, 409–431.
2. Jin, R. C. Quantum Sized, Thiolate-Protected Gold Nanoclusters. *Nanoscale* **2010**, *2*, 343–362.
3. Lin, C. A. J.; Lee, C. H.; Hsieh, J. T.; Wang, H. H.; Li, J. K.; Shen, J. L.; Chan, W. H.; Yeh, H. I.; Chang, W. H. Synthesis of Fluorescent Metallic Nanoclusters toward Biomedical Application: Recent Progress and Present Challenges. *J. Med. Biol. Eng.* **2009**, *29*, 276–283.
4. Xu, H.; Suslick, K. S. Water-Soluble Fluorescent Silver Nanoclusters. *Adv. Mater.* **2010**, *22*, 1078–1082.
5. Diez, I.; Ras, R. H. A. Fluorescent Silver Nanoclusters. *Nanoscale* **2011**, *3*, 1963–1970.
6. Richards, C. I.; Choi, S.; Hsiang, J. C.; Antoku, Y.; Vosch, T.; Bongiorno, A.; Tzeng, Y. L.; Dickson, R. M. Oligonucleotide-Stabilized Ag Nanocluster Fluorophores. *J. Am. Chem. Soc.* **2008**, *130*, 5038–5039.
7. Ramakrishna, G.; Varnavski, O.; Kim, J.; Lee, D.; Goodson, T. Quantum-Sized Gold Clusters as Efficient Two-Photon Absorbers. *J. Am. Chem. Soc.* **2008**, *130*, 5032–5033.
8. Patel, S. A.; Richards, C. I.; Hsiang, J. C.; Dickson, R. M. Water-Soluble Ag Nanoclusters Exhibit Strong Two-Photon-Induced Fluorescence. *J. Am. Chem. Soc.* **2008**, *130*, 11602–11603.
9. Vosch, T.; Antoku, Y.; Hsiang, J. C.; Richards, C. I.; Gonzalez, J. I.; Dickson, R. M. Strongly Emissive Individual DNA-Encapsulated Ag Nanoclusters as Single-Molecule Fluorophores. *Proc. Natl. Acad. Sci. U.S.A.* **2007**, *104*, 12616–12621.
10. Gonzalez, J. I.; Vosch, T.; Dickson, R. M. Charge Injection into Discrete States of Individual Electroluminescent Au Nanoclusters. *Phys. Rev. B* **2006**, *74*, 064305.
11. Lee, T. H.; Gonzalez, J. I.; Dickson, R. M. Strongly Enhanced Field-Dependent Single-Molecule Electroluminescence. *Proc. Natl. Acad. Sci. U.S.A.* **2002**, *99*, 10272–10275.
12. Haynes, C. L.; McFarland, A. D.; Zhao, L. L.; Van Duyne, R. P.; Schatz, G. C.; Gunnarsson, L.; Prikulis, J.; Kasemo, B.; Kall, M. Nanoparticle Optics: The Importance of Radiative Dipole Coupling in Two-Dimensional Nanoparticle Arrays. *J. Phys. Chem. B* **2003**, *107*, 7337–7342.
13. Kawasaki, H.; Yoshimura, K.; Hamaguchi, K.; Arakawa, R. Trypsin-Stabilized Fluorescent Gold Nanocluster for Sensitive and Selective Hg^{2+} Detection. *Anal. Sci.* **2011**, *27*, 591–596.
14. Durgadas, C. V.; Sharma, C. P.; Sreenivasan, K. Fluorescent Gold Clusters as Nanosensors for Copper Ions in Live Cells. *Analyst* **2011**, *136*, 933–940.
15. Lan, G. Y.; Huang, C. C.; Chang, H. T. Silver Nanoclusters as Fluorescent Probes for Selective and Sensitive Detection of Copper Ions. *Chem. Commun.* **2010**, *46*, 1257–1259.
16. Wang, M.; Mei, Q. S.; Zhang, K.; Zhang, Z. P. Protein-Gold Nanoclusters for Identification of Amino Acids by Metal Ions Modulated Ratiometric Fluorescence. *Analyst* **2012**, *137*, 1618–1623.
17. Haruta, M. Catalysis: Gold Rush. *Nature* **2005**, *437*, 1098–1099.
18. Zhu, Y.; Qian, H.; Drake, B. A.; Jin, R. Atomically Precise $Au_{25}(SR)_{18}$ Nanoparticles as Catalysts for the Selective Hydrogenation of α,β-Unsaturated Ketones and Aldehydes. *Angew. Chem., Int. Ed.* **2010**, *49*, 1295–1298.
19. Liu, Y. M.; Tsunoyama, H.; Akita, T.; Tsukuda, T. Efficient and Selective Epoxidation of Styrene with TBHP Catalyzed By Au_{25} Clusters on Hydroxyapatite. *Chem. Commun.* **2010**, *46*, 550–552.

20. Leelavathi, A.; Rao, T. U. B.; Pradeep, T. Supported Quantum Clusters of Silver as Enhanced Catalysts for Reduction. *Nanoscale Res. Lett.* **2011**, *6*, 1–9.
21. Lin, C. A.; Yang, T. Y.; Lee, C. H.; Huang, S. H.; Sperling, R. A.; Zanella, M.; Li, J. K.; Shen, J. L.; Wang, H. H.; Yeh, H. C.; *et al.* Synthesis, Characterization, and Bioconjugation of Fluorescent Gold Nanoclusters toward Biological Labeling Applications. *ACS Nano* **2009**, *3*, 395–401.
22. Muhammed, M. A. H.; Verma, P. K.; Pal, S. K.; Kumar, R. C. A.; Paul, S.; Omkumar, R. V.; Pradeep, T. Bright, NIR-Emitting Au_{23} from Au_{25}: Characterization and Applications Including Biolabeling. *Chem.—Eur. J.* **2009**, *15*, 10110–10120.
23. Muhammed, M. A. H.; Verma, P. K.; Pal, S. K.; Retnakumari, A.; Koyakutty, M.; Nair, S.; Pradeep, T. Luminescent Quantum Clusters of Gold in Bulk by Albumin-Induced Core Etching of Nanoparticles: Metal Ion Sensing, Metal-Enhanced Luminescence, and Biolabeling. *Chem.—Eur. J.* **2010**, *16*, 10103–10112.
24. Retnakumari, A.; Setua, S.; Menon, D.; Ravindran, P.; Muhammed, H.; Pradeep, T.; Nair, S.; Koyakutty, M. Molecular-Receptor-Specific, Non-toxic, Near-Infrared-Emitting Au Cluster-Protein Nanoconjugates for Targeted Cancer Imaging. *Nanotechnology* **2010**, *21*, 055103.
25. Retnakumari, A.; Jayasimhan, J.; Chandran, P.; Menon, D.; Nair, S.; Mony, U.; Koyakutty, M. CD33 Monoclonal Antibody Conjugated Au Cluster Nano-Bioprobe for Targeted Flow-Cytometric Detection of Acute Myeloid Leukaemia. *Nanotechnology* **2011**, *22*, 285102(1−11).
26. Yu, J. H.; Choi, S.; Dickson, R. M. Shuttle-Based Fluorogenic Silver-Cluster Biolabels. *Angew. Chem., Int. Ed.* **2009**, *48*, 318–320.
27. Wu, X.; He, X. X.; Wang, K. M.; Xie, C.; Zhou, B.; Qing, Z. H. Ultrasmall Near-Infrared Gold Nanoclusters for Tumor Fluorescence Imaging *in Vivo*. *Nanoscale* **2010**, *2*, 2244–2249.
28. Wang, Y. L.; Chen, J. J.; Irudayaraj, J. Nuclear Targeting Dynamics of Gold Nanoclusters for Enhanced Therapy of $HER2^+$ Breast Cancer. *ACS Nano* **2011**, *5*, 9718–9725.
29. Wang, C. S.; Li, J. Y.; Amatore, C.; Chen, Y.; Jiang, H.; Wang, X. M. Gold Nanoclusters and Graphene Nanocomposites for Drug Delivery and Imaging of Cancer Cells. *Angew. Chem., Int. Ed.* **2011**, *50*, 11644–11648.
30. Wang, Y.; Zhang, J.; Huang, L.; He, D.; Ma, L.; Ouyang, J.; Jiang, F. Novel Application of Ag Nanoclusters in Fluorescent Imaging of Human Serum Proteins after Native Polyacrylamide Gel Electrophoresis (PAGE). *Chemistry* **2012**, *18*, 1432–1437.
31. Ai, J.; Guo, W.; Li, B.; Li, T.; Li, D.; Wang, E. DNA G-Quadruplex-Templated Formation of the Fluorescent Silver Nanocluster and Its Application to Bioimaging. *Talanta* **2012**, *88*, 450–455.
32. Pelley, J. L.; Daar, A. S.; Saner, M. A. State of Academic Knowledge on Toxicity and Biological Fate of Quantum Dots. *Toxicol. Sci.* **2009**, *112*, 276–296.
33. Mattoussi, H.; Palui, G.; Na, H. B. Luminescent Quantum Dots as Platforms for Probing *In Vitro* and *In Vivo* Biological Processes. *Adv. Drug Delivery Rev.* **2012**, *64*, 138–166.
34. Ye, L.; Yong, K.-T.; Liu, L.; Roy, I.; Hu, R.; Zhu, J.; Cai, H.; Law, W.-C.; Liu, J.; Wang, K.; *et al.* A Pilot Study in Non-Human Primates Shows No Adverse Response to Intravenous Injection of Quantum Dots. *Nat. Nanotechnol.* **2012**, *7*, 453–458.
35. Linnert, T.; Mulvaney, P.; Henglein, A.; Weller, H. Long-Lived Nonmetallic Silver Clusters in Aqueous-Solution—Preparation and Photolysis. *J. Am. Chem. Soc.* **1990**, *112*, 4657–4664.
36. Peyser, L. A.; Vinson, A. E.; Bartko, A. P.; Dickson, R. M. Photoactivated Fluorescence from Individual Silver Nanoclusters. *Science* **2001**, *291*, 103–106.
37. Zheng, J.; Dickson, R. M. Individual Water-Soluble Dendrimer-Encapsulated Silver Nanodot Fluorescence. *J. Am. Chem. Soc.* **2002**, *124*, 13982–13983.
38. Zhang, J. G.; Xu, S. Q.; Kumacheva, E. Photogeneration of Fluorescent Silver Nanoclusters in Polymer Microgels. *Adv. Mater.* **2005**, *17*, 2336–2340.
39. Shang, L.; Dong, S. J. Facile Preparation of Water-Soluble Fluorescent Silver Nanoclusters Using a Polyelectrolyte Template. *Chem. Commun.* **2008**, 1088–1090.
40. Xu, H. X.; Suslick, K. S. Sonochemical Synthesis of Highly Fluorescent Ag Nanoclusters. *ACS Nano* **2010**, *4*, 3209–3214.
41. Petty, J. T.; Zheng, J.; Hud, N. V.; Dickson, R. M. DNA-Templated Ag Nanocluster Formation. *J. Am. Chem. Soc.* **2004**, *126*, 5207–5212.
42. Wu, Z.; Lanni, E.; Chen, W.; Bier, M. E.; Ly, D.; Jin, R. High Yield, Large Scale Synthesis of Thiolate-Protected Ag_7 Clusters. *J. Am. Chem. Soc.* **2009**, *131*, 16672–16674.
43. Adhikari, B.; Banerjee, A. Facile Synthesis of Water-Soluble Fluorescent Silver Nanoclusters and Hg(II) Sensing. *Chem. Mater.* **2010**, *22*, 4364–4371.
44. Rao, T. U. B.; Nataraju, B.; Pradeep, T. Ag_9 Quantum Cluster through a Solid-State Route. *J. Am. Chem. Soc.* **2010**, *132*, 16304–16307.
45. Guo, W. W.; Yuan, J. P.; Dong, Q. Z.; Wang, E. K. Highly Sequence-Dependent Formation of Fluorescent Silver Nanoclusters in Hybridized DNA Duplexes for Single Nucleotide Mutation Identification. *J. Am. Chem. Soc.* **2010**, *132*, 932–934.
46. Guo, C. L.; Irudayaraj, J. Fluorescent Ag Clusters *via* a Protein-Directed Approach as a Hg(II) Ion Sensor. *Anal. Chem.* **2011**, *83*, 2883–2889.
47. Gwinn, E. G.; O'Neill, P.; Guerrero, A. J.; Bouwmeester, D.; Fygenson, D. K. Sequence-Dependent Fluorescence of DNA-Hosted Silver Nanoclusters. *Adv. Mater.* **2008**, *20*, 279–283.
48. Sengupta, B.; Ritchie, C. M.; Buckman, J. G.; Johnsen, K. R.; Goodwin, P. M.; Petty, J. T. Base-Directed Formation of Fluorescent Silver Clusters. *J. Phys. Chem. C* **2008**, *112*, 18776–18782.
49. Yeh, H. C.; Sharma, J.; Han, J. J.; Martinez, J. S.; Werner, J. H. A DNA-Silver Nanocluster Probe That Fluoresces upon Hybridization. *Nano Lett.* **2010**, *10*, 3106–3110.
50. Yu, J.; Patel, S. A.; Dickson, R. M. *In Vitro* and Intracellular Production of Peptide-Encapsulated Fluorescent Silver Nanoclusters. *Angew. Chem., Int. Ed.* **2007**, *46*, 2028–2030.
51. Cui, Y. Y.; Wang, Y. L.; Liu, R.; Sun, Z. P.; Wei, Y. T.; Zhao, Y. L.; Gao, X. Y. Serial Silver Clusters Biomineralized by One Peptide. *ACS Nano* **2011**, *5*, 8684–8689.
52. Mathew, A.; Sajanlal, P. R.; Pradeep, T. A Fifteen Atom Silver Cluster Confined in Bovine Serum Albumin. *J. Mater. Chem.* **2011**, *21*, 11205–11212.
53. Mrudula, K. V.; Rao, T. U. B.; Pradeep, T. Interfacial Synthesis of Luminescent 7 kDa Silver Clusters. *J. Mater. Chem.* **2009**, *19*, 4335–4342.
54. Udaya Bhaskara Rao, T.; Pradeep, T. Luminescent Ag_7 and Ag_8 Clusters by Interfacial Synthesis. *Angew. Chem., Int. Ed.* **2010**, *49*, 3925–3929.
55. Cathcart, N.; Mistry, P.; Makra, C.; Pietrobon, B.; Coombs, N.; Jelokhani-Niaraki, M.; Kitaev, V. Chiral Thiol-Stabilized Silver Nanoclusters with Well-Resolved Optical Transitions Synthesized by a Facile Etching Procedure in Aqueous Solutions. *Langmuir* **2009**, *25*, 5840–5846.
56. Nishida, N.; Yao, H.; Ueda, T.; Sasaki, A.; Kimura, K. Synthesis and Chiroptical Study of D/L-Penicillamine-Capped Silver Nanoclusters. *Chem. Mater.* **2007**, *19*, 2831–2841.
57. Dhanalakshmi, L.; Udayabhaskararao, T.; Pradeep, T. Conversion of Double Layer Charge-Stabilized Ag@Citrate Colloids to Thiol Passivated Luminescent Quantum Clusters. *Chem. Commun.* **2012**, *48*, 859–861.
58. Yuan, X.; Luo, Z. T.; Zhang, Q. B.; Zhang, X. H.; Zheng, Y. G.; Lee, J. Y.; Xie, J. P. Synthesis of Highly Fluorescent Metal (Ag, Au, Pt, and Cu) Nanoclusters by Electrostatically Induced Reversible Phase Transfer. *ACS Nano* **2011**, *5*, 8800–8808.
59. Huang, Z.; Pu, F.; Lin, Y.; Ren, J.; Qu, X. Modulating DNA-Templated Silver Nanoclusters for Fluorescence Turn-On Detection of Thiol Compounds. *Chem. Commun.* **2011**, *47*, 3487–3489.
60. Liu, S.; Lu, F.; Zhu, J. J. Highly Fluorescent Ag Nanoclusters: Microwave-Assisted Green Synthesis And Cr^{3+} Sensing. *Chem. Commun.* **2011**, *47*, 2661–2663.

61. Su, Y. T.; Lan, G. Y.; Chen, W. Y.; Chang, H. T. Detection of Copper Ions through Recovery of the Fluorescence of DNA-Templated Copper/Silver Nanoclusters in the Presence of Mercaptopropionic Acid. *Anal. Chem.* **2010**, *82*, 8566–8572.
62. Sharma, J.; Yeh, H. C.; Yoo, H.; Werner, J. H.; Martinez, J. S. Silver Nanocluster Aptamers: *In Situ* Generation of Intrinsically Fluorescent Recognition Ligands for Protein Detection. *Chem. Commun.* **2011**, *47*, 2294–2296.
63. Negishi, Y.; Nobusada, K.; Tsukuda, T. Glutathione-Protected Gold Clusters Revisited: Bridging the Gap between Gold(I)−Thiolate Complexes and Thiolate-Protected Gold Nanocrystals. *J. Am. Chem. Soc.* **2005**, *127*, 5261–5270.
64. Xie, J. P.; Zheng, Y. G.; Ying, J. Y. Protein-Directed Synthesis of Highly Fluorescent Gold Nanoclusters. *J. Am. Chem. Soc.* **2009**, *131*, 888–889.
65. Uyeda, H. T.; Medintz, I. L.; Jaiswal, J. K.; Simon, S. M.; Mattoussi, H. Synthesis of Compact Multidentate Ligands To Prepare Stable Hydrophilic Quantum Dot Fluorophores. *J. Am. Chem. Soc.* **2005**, *127*, 3870–3878.
66. Susumu, K.; Uyeda, H. T.; Medintz, I. L.; Pons, T.; Delehanty, J. B.; Mattoussi, H. Enhancing the Stability and Biological Functionalities of Quantum Dots *via* Compact Multifunctional Ligands. *J. Am. Chem. Soc.* **2007**, *129*, 13987–13996.
67. Oh, E.; Susumu, K.; Goswami, R.; Mattoussi, H. One-Phase Synthesis of Water-Soluble Gold Nanoparticles with Control over Size and Surface Functionalities. *Langmuir* **2010**, *26*, 7604–7613.
68. Stewart, M. H.; Susumu, K.; Mei, B. C.; Medintz, I. L.; Delehanty, J. B.; Blanco-Canosa, J. B.; Dawson, P. E.; Mattoussi, H. Multidentate Poly(ethylene glycol) Ligands Provide Colloidal Stability to Semiconductor and Metallic Nanocrystals in Extreme Conditions. *J. Am. Chem. Soc.* **2010**, *132*, 9804–9813.
69. Susumu, K.; Mei, B. C.; Mattoussi, H. Multifunctional Ligands Based on Dihydrolipoic Acid and Polyethylene Glycol To Promote Biocompatibility of Quantum Dots. *Nat. Protoc.* **2009**, *4*, 424–436.
70. Dougherty, R. C. Temperature and Pressure Dependence of Hydrogen Bond Strength: A Perturbation Molecular Orbital Approach. *J. Chem. Phys.* **1998**, *109*, 7372–7378.
71. Peng, S.; McMahon, J. M.; Schatz, G. C.; Gray, S. K.; Sun, Y. G. Reversing the Size-Dependence of Surface Plasmon Resonances. *Proc. Natl. Acad. Sci. U.S.A.* **2010**, *107*, 14530–14534.
72. Zhu, M.; Aikens, C. M.; Hollander, F. J.; Schatz, G. C.; Jin, R. Correlating the Crystal Structure of a Thiol-Protected Au-25 Cluster and Optical Properties. *J. Am. Chem. Soc.* **2008**, *130*, 5883–5885.
73. Bakr, O. M.; Amendola, V.; Aikens, C. M.; Wenseleers, W.; Li, R.; Dal Negro, L.; Schatz, G. C.; Stellacci, F. Silver Nanoparticles with Broad Multiband Linear Optical Absorption. *Angew. Chem., Int. Ed.* **2009**, *48*, 5921–5926.
74. Bae, G. T.; Aikens, C. M. Time-Dependent Density Functional Theory Studies of Optical Properties of Ag Nanoparticles: Octahedra, Truncated Octahedra, and Icosahedra. *J. Phys. Chem. C* **2012**, *116*, 10356–10367.
75. Aikens, C. M. Origin of Discrete Optical Absorption Spectra of $M_{25}(SH)_{18}^-$ Nanoparticles (M = Au, Ag). *J. Phys. Chem. C* **2008**, *112*, 19797–19800.
76. Chestnoy, N.; Harris, T. D.; Hull, R.; Brus, L. E. Luminescence and Photophysics of Cadmium Sulfide Semiconductor Clusters: The Nature of the Emitting Electronic State. *J. Phys. Chem.* **1986**, *90*, 3393–3399.
77. (a) Bucher, G.; Lu, C. Y.; Sander, W. The Photochemistry of Lipoic Acid: Photoionization and Observation of a Triplet Excited State of a Disulfide. *ChemPhysChem* **2005**, *6*, 2607–2618. (b) Palui, G.; Avellini, T.; Zhan, N.; Feng, P.; Gray, D. L.; Alabugin, I.; Mattoussi, H. Photo-induced Ligand Exchange and Phase Transfer of Luminescent Quantum Dots to Aqueous Media. *J. Am. Chem. Soc.* **2012**, DOI: 10.1021/ja306621n.
78. Shichibu, Y.; Negishi, Y.; Tsunoyama, H.; Kanehara, M.; Teranishi, T.; Tsukuda, T. Extremely High Stability of Glutathionate-Protected Au_{25} Clusters Against Core Etching. *Small* **2007**, *3*, 835–839.
79. Wu, Z.; MacDonald, M. A.; Chen, J.; Zhang, P.; Jin, R. Kinetic Control and Thermodynamic Selection in the Synthesis of Atomically Precise Gold Nanoclusters. *J. Am. Chem. Soc.* **2011**, *133*, 9670–9673.
80. Jin, R. C.; Qian, H. F.; Wu, Z. K.; Zhu, Y.; Zhu, M. Z.; Mohanty, A.; Garg, N. Size Focusing: A Methodology for Synthesizing Atomically Precise Gold Nanoclusters. *J. Phys. Chem. Lett.* **2010**, *1*, 2903–2910.
81. Aslan, K.; Wu, M.; Lakowicz, J. R.; Geddes, C. D. Fluorescent Core−Shell Ag@SiO_2 Nanocomposites for Metal-Enhanced Fluorescence and Single Nanoparticle Sensing Platforms. *J. Am. Chem. Soc.* **2007**, *129*, 1524–1525.
82. Qian, H. F.; Zhu, M. Z.; Lanni, E.; Zhu, Y.; Bier, M. E.; Jin, R. C. Conversion of Polydisperse Au Nanoparticles into Monodisperse Au_{25} Nanorods and Nanospheres. *J. Phys. Chem. C* **2009**, *113*, 17599–17603.
83. Mei, B. C.; Susumu, K.; Medintz, I. L.; Delehanty, J. B.; Mountziaris, T. J.; Mattoussi, H. Modular Poly(ethylene glycol) Ligands for Biocompatible Semiconductor and Gold Nanocrystals with Extended pH and Ionic Stability. *J. Mater. Chem.* **2008**, *18*, 4949–4958.
84. Qian, H.; Zhu, Y.; Jin, R. Size-Focusing Synthesis, Optical and Electrochemical Properties of Monodisperse $Au_{38}(SC_2H_4Ph)_{24}$ Nanoclusters. *ACS Nano* **2009**, *3*, 3795–3803.